Buried Pipe Axial Displacement due to Temperature and Pressure Change

Mark C Gemperline, Ph.D., P.E., M.ASCE

President, MCG Geotechnical Engineering Inc.

Abstract

A mathematical solution is presented that describes both axial wall stress and axial displacement of buried pipe subject to temperature and pressure change with axial displacement resisted only by friction at the embedment interface. A simple model and its mathematical solution are developed to clarify the way a pipe transfers load to the surrounding embedment. Equations are derived for maximum pipe wall axial stress and maximum pipe displacement at the free ends of an infinitely long buried pipe. Dimensional analysis is used to reduce the number of independent variables. The results advance understanding of buried pipe behavior and provides a basis for additional research. Limitations regarding use of the derived equations are discussed.

Buried Pipe Axial Displacement due to Temperature and Pressure Change

Introduction

Methods for calculating the magnitude of unrestrained expansion and contraction of materials due to temperature and pressure change are taught in engineering courses and derived in commonly used text. These methods are often applied to calculate axial displacement of unrestrained pipe due to changes in temperature and both internal and external pressures. However, axial displacement of a buried pipe is partially restrained by friction that develops at the pipe-embedment interface. A mathematical expression describing axial displacement of pipe under this condition is developed herein to support better understanding of buried pipe behavior and facilitate additional research.

The ASCE Task Committee on Thrust Restraint Design for Buried Pipelines recognized the need for a mathematical description of this problem (ASCE 2014). The committee suggested that the relationship between frictional resistance and displacement at the pipe-embedment interface must be similar to that derived by geotechnical engineers for the purpose of approximating pile foundation vertical displacement. Approximate closed-form solutions that describe axial displacement of piles have been developed by Randolph and Wroth (Randolph and Wroth 1978) and Motta (Motta 1994). Their solutions assume linear elastic behavior of the pile and elastic perfectly plastic behavior of adjacent soil. Such mathematical formulations helped clarify how foundation piles transfer load to the surrounding soil. These concepts, with modifications, are used herein to develop equations that describe buried pipe axial displacement and pipe wall axial stress caused by both temperature and pressure changes. The solution is then used to derive an expression for the limiting axial displacement at the free end of an infinitely long buried pipe due to temperature and pressure change. The solution confirms the intuitive expectation that the maximum pipe wall stress in a buried pipe that is not restrained at both ends and experiences temperature and pressure change is less than the value calculated for a pipe restrained at both ends. Variables are reduced to dimensionless form and a chart that presents relationships between problem variables is presented. Finally, application and limitations regarding the use of derived equations are discussed.

Problem Statement

A simple model of a buried pipe is used to facilitate the development of a mathematical solution. Figure 1 illustrates the conceptual problem. A horizontal pipe of constant cross-section and length 2α experiences normal and shear stresses that act uniformly about its circumference at the pipe-embedment interface. The pipe expands or contracts axially due to temperature or pressure change resulting in shear stress that varies along the pipe length. Normal stress acting on the pipe-embedment interface is herein presumed uniform along the entire length of pipe for mathematical convenience.

Initially, there is no shear stress at the pipe-embedment interface. Shear stress at the pipe-embedment interface develops in response to axis-symmetric axial displacement caused by temperature change, ΔT, change in external total stress acting normal to the circumference, ΔQ, and change in internal pipe pressure, ΔP. Individually or acting together, ΔT, ΔQ and ΔP cause the pipe to expand or contract both

radially and axially. There are no caps or restraints at either end of the conceptual pipe. Frictional resistance that develops along the pipe-embedment interface is the only force opposing pipe axial displacement. A mathematical solution that approximately describes axial displacement for buried pipe experiencing ΔT, ΔQ and ΔP is derived.

Simplifying assumptions are made to facilitate the mathematical solution. Both the pipe and embedment materials are presumed to be linear elastic, homogeneous and isotropic. Pipe wall strain due to temperature change is linearly proportional to ΔT. Body forces are not considered. Shear and normal stresses acting at the pipe-embedment interface are axis-symmetric. Also, it is presumed that initially no shear or axial stresses act on or in the pipe wall. A stick-slip model is used to describe pipe-embedment interface friction. The stick-slip model is described in the next section. Additional simplifying assumptions are introduced in subsequent discussion as they are applied.

The problem is two-dimensional since a pipe subject to changes ΔT, ΔQ and ΔP must expand or contract both radially and axially. However, for mathematical convenience, an expression is derived for the one-dimensional axial displacement condition. Hence, functions relating pipe-embedment interface normal and shear stress to radial expansion or contraction of the pipe are not included in the derivation.

Geometric symmetry about the pipe centerline allows simplification of the problem. As seen in Figure 1. The pipe has length 2a. The horizontal distance from the center of the pipe, x, is positive to the right of centerline and negative to the left. ΔT, ΔQ and ΔP will not result in axial displacement at x=0 due to symmetry. Additionally, functions representing embedment-pipe interface axial shear stress τ(x), pipe axial displacement, δ(x), and pipe-wall axial stress, σ(x), are expected to be symmetric about x=0. The symmetry of these functions is exemplified by graphs presented on Figure 2. Due to this symmetry, a solution that describes τ(x), δ(x) and σ(x) for positive values of x is sufficient to completely describe the problem.

Expectedly, the plots of τ(x), δ(x) and σ(x) are mirrored about the x-axis for conditions of pipe expansion and contraction as shown on Figure 2. This results from two conceptual model conditions. First, is the condition that, τ(x), δ(x) and σ(x) are zero prior to application of ΔT, ΔQ and ΔP. Second, materials are modeled to be linear thermoelastic and exhibit linear response to temperature and pressure change. Consequently, a complete solution may be represented by the solution to either the pipe expansion or contraction condition. Therefore, for convenience, the solution is developed herein only for the conditions of ΔT, ΔQ and ΔP that result in pipe expansion.

Figure 3 presents the problem to be solved for the expanding pipe right of centerline, i.e. positive x, τ(x), δ(x) and σ(x) values. The left end, x=0, is “fixed” and the right end, x=a, is “free”. The boundary conditions at the ends of the pipe are: $\delta(0) = 0$, $d\sigma(0)/dx = 0$, and $\sigma(a) = 0$.

Shear stress is presumed to increase linearly in the region $0 \le x < b$ with $\tau(0)=0$ and $\tau(b)= \tau_m$. Shear stress is constant and of magnitude τ_m in the region $b \le x \le a$. Consequently, a discontinuity is present at x=b where $\delta(b) = \delta_m$. Graphs depicting a set of possible functions of τ(x), δ(x) and σ(x) are presented on Figure 4. These graphs were created using the subsequently developed solution for conditions discussed later in this paper.

Pipe-Embedment Interface Shear Behavior

Figure 4 shows τ(x) increasing in magnitude with increasing x in the region 0≤x≤b and constant in the region b≤x≤a. The discontinuity at x=b is a consequence of assuming a stick-slip model to represent the friction that develops on the pipe-embedment interface. The stick-slip model for the pipe-embedment interface friction behavior is portrayed on Figure 5 and described by the following equations.

$$\tau(x) = \delta(x)\psi \quad \text{for } \delta(x) < \delta_m \qquad 1$$

$$\tau_m = \delta_m\psi \qquad \text{for } \delta(x) \geq \delta_m \qquad 2$$

Where

$\tau(x)$ = pipe-embedment interface shear stress at x.

$\delta(x)$ = pipe axial displacement at x.

δ_m= magnitude of pipe axial displacement required to mobilize τ_m.

τ_m= maximum pipe-embedment interface frictional resistance.

$\psi = \tau_m/\delta_m$.

Herein, b is termed the development length and is the least value of x at which the pipe has moved sufficiently to achieve τ_m. The mathematical solution developed herein presumes the pipe length is greater than the development length, i.e. a≥b.

The pipe behavior in the regions 0≤x<b and b≤x≤a have the following interpretations:

- 0≤x<b: the embedment adjacent to the pipe moves with the pipe as the pipe displaces axially in response to ΔT, ΔQ and ΔP. In other words, the embedment seemingly sticks to the pipe. The shear stress at the pipe-embedment interface increases linearly with displacement and occurs concurrently with the development of embedment shear strain.
- b≤x≤a: The pipe has displaced axially a sufficient distance in response to changes in ΔT, ΔQ and ΔP to achieve τ_m at the pipe-embedment interface. The pipe slips past the embedment with constant shear stress, τ_m.

Values that best represent variables τ_m and δ_m depend, among other things, on embedment properties, pipe-embedment interface frictional characteristics, history of pipe expansion and contraction, and pipe-embedment geometric variables. The hypothetical τ(x) v. δ(x) plot, with a limiting value of τ_m, is analogous to the bilinear t-z curve proposed by Motta in his development of an approximate closed-form solution for the displacement of axially loaded piles (Motta, 1994). Motta stated, “Procedures for the evaluation of t-z curves are mainly empirical, however some theoretical basis has been given (Kraft et al. 1981).”

Different sets of equations are needed to describe pipe behavior and pipe-embedment interaction on either side of the discontinuity at x=b. These equations are developed herein. Equilibrium, conditions of continuity and compatibility and boundary conditions are used to derive the problem solution.

Figures 6a and 6b separate the problem into two parts that are characterized by $0 \le x < b$ and $b \le x \le a$. Different boundary conditions apply to these pipe segments. Hence, these pipe segments are treated separately in subsequent development of a mathematical solution.

One-Dimensional Representation of the Problem

A one-dimensional model is developed to simplify derivation of a mathematical solution. The circular pipe is herein modeled as a horizontal plate of uniform thickness and having a width equal to the outside circumference. This is illustrated in cross-sections on Figures 7a and 7b. The length of the plate is equal to the length of the pipe, the width of the plate is equal to the outside circumference of the pipe, and the cross-sectional area of the plate is equal to the cross-sectional area of the pipe wall. Friction develops on only one side of the plate to appropriately represent friction developing only on the outside of a pipe.

The cross-sectional area of the pipe wall and hypothetical plate are equal. To ensure this, the transformed thickness, t, of the hypothetical plate is the pipe cross-section wall area, A, divided by the pipe external circumference.

$$t = \frac{A}{\pi D_2} \qquad 3$$

Where:

A = pipe wall cross-sectional area.

D_2 = pipe outside diameter.

This transformation of pipe wall thickness simplifies subsequent calculations while appropriately maintaining important pipe problem characteristics. Comparing the circular pipe to the one-dimensional plate model: shear stress at the pipe-embedment interface acts on equal surface areas resulting in the same values for axial force; and the axial force is divided by equal cross-sectional area resulting in the same axial stresses. Axial stress is presumed to develop uniformly and equally within both the plate and pipe wall due to the contribution of shear stress on one surface. The equality of both surface and cross-sectional areas for the plate and pipe ensures equivalent axial stress. A unit width of the transformed pipe is used in subsequent problem development.

Thermal and Pressure Effects

The component of pipe axial strain due to ΔT, ΔQ and ΔP, ε_1, is constant along the length of the pipe and is approximated by (Boresi and Sidebottom 1985):

- $\varepsilon_1=C\Delta T -2\nu/E\ (\Delta Q\ D_2^2-\Delta P\ D_1^2)/\ (D_2^2-D_1^2)$ 4

where:

- E and ν are the Young's modulus and Poisson ratio for the pipe wall material.
- D_1 and D_2 are the pipe inside and outside diameters respectively.
- C is the coefficient of linear thermal expansion.
- Strain resulting in increased pipe length is positive strain.

Pipe Wall Stress-Strain Behavior

The component of pipe wall axial strain, $\varepsilon_2(x)$, caused by pipe wall axial stress, σ(x) is approximated by:

- $\varepsilon_2(x) = \frac{\sigma(x)}{E}$ 5
- Herein, pipe wall compressive stress and associated strain are positive.

Solution

Initially, the general equations describing relationships between stress, strain and displacement are defined. This is followed by independent development of the governing equations for pipe segments left and right of the discontinuity at x= b.

The rate of change of axial displacement with respect to x is:

$$\frac{d}{dx}\delta(x) = \varepsilon_1 - \varepsilon_2(x) \quad 6$$

Figure 8 is a free-body diagram for an infinitesimal length, dx, of a unit width of transformed pipe wall having transformed thickness, t.

Horizontal force equilibrium on segment dx leads to the following expression.

$$\frac{d}{dx}\sigma(x) = -\frac{\tau(x)}{t} \quad 7$$

Substituting Eq. 5 into Eq. 6 yields.

$$\frac{d}{dx}\delta(x) = \varepsilon_1 - \frac{\sigma(x)}{E} \quad 8$$

Develop problem for 0≤x<b

Substitute Eq. 1 into Eq. 7.

$$\frac{d}{dx}\sigma(x) = \frac{-\delta(x)\psi}{t} \quad (9)$$

Differentiate Eq. 9 with respect to x.

$$\frac{d^2}{dx^2}\sigma(x) = \frac{-\psi}{t}\left\{\frac{d}{d(x)}\delta(x)\right\} \quad (10)$$

Substitute Eq. 8 into Eq. 10.

$$\frac{d^2}{dx^2}\sigma(x) = \frac{-\psi}{t}\left\{\varepsilon_1 - \frac{\sigma(x)}{E}\right\} \quad (11)$$

Rearrange Eq. 11.

$$\frac{d^2}{dx^2}\sigma(x) - \frac{\psi}{Et}\sigma(x) = \frac{-\psi}{t}\{\varepsilon_1\} \quad (12)$$

The general solution to Eq. 12 is

$$\sigma(x) = C_1 e^{kx} + C_2 e^{-kx} + \varepsilon_1 E \quad (13)$$

where

$$k = \sqrt{\frac{\psi}{Et}}$$

and C_1 and C_2 are constants. (14)

Differentiate equation 13.

$$\frac{d\sigma(x)}{dx} = C_1 k\, e^{kx} - C_2 k\, e^{-kx} \quad (15)$$

Substitute 13 into 8.

$$\frac{d}{dx}\delta(x) = \varepsilon_1 - \frac{C_1 e^{kx} + C_2 e^{-kx} + \varepsilon_1 E}{E} \quad (16)$$

Rearrange 16 and integrate between x= 0 and x.

$$\delta(x) = \frac{C_1 kt(1-e^{kx}) - C_2 kt(1-e^{-kx})}{\psi} + C_3 \quad (17)$$

where C_3 is introduced as an integration constant.

Develop problem for b≤x≤a

By problem definition $\tau(x) = \tau_m$ in the region *for b≤x≤a.*

Substitute Eq. 2 into Eq. 7

$$\frac{d\sigma(x)}{dx} = \frac{-\tau_m}{t} \quad (18)$$

Rearrange Eq. 18 and integrate between b and x

$$\sigma(x) = \frac{-\tau_m}{t}(x-b) + C_4 \quad 19$$

where C_4 is introduced as an integration constant.

Substitute Eq. 19 into Eq. 8

$$\frac{d}{dx}\delta(x) = \varepsilon_1 - \frac{\frac{-\tau_m}{t}(x-b)+C_4}{E} \quad 20$$

Rearrange Eq. 20 and integrate between the limits b and x

$$\delta(x) = \frac{\tau_m}{2Et}(x-b)^2 - \frac{C_4 - E\varepsilon_1}{E}(x-b) + C_5 \quad 21$$

where C_5 is introduced as an integration constant.

Solve for Constants

Boundary and compatibility/continuity conditions are used to solve for constants C1 through C5.

Apply the boundary condition δ(0) = 0 to Eq. 17.

$$C_3 = 0 \quad 22$$

Apply the boundary condition, σ(a)=0 to Eq. 19 .

$$C_4 = \frac{\tau_m}{t}(a-b) \quad 23$$

Apply the boundary condition δ(b) = δ_m to Eq.21.

$$C_5 = \delta_m \quad 24$$

Equate Eq. 13 and Eq. 19 to ensure pipe wall axial stress compatibility at x=b. Solve for C_1.

$$C_1 = e^{-kb}\left(\frac{(a-b)\tau_m}{\mathrm{t}} - E\varepsilon_1 - C_2 e^{-kb}\right) \quad 25$$

Equate Eq. 17 and Eq. 21 to ensure axial displacement compatibility at x=b. Solve for C_2.

$$C_2 = \frac{k((a-b)\tau_m - E\varepsilon_1 t)\left(e^{-kb}-1\right) - \psi\delta_m}{kt\left(e^{-kb}-1\right)^2} \quad 26$$

Solve for development length (b)

Apply the boundary condition dσ(0)/dx=0 to Eq. 15 and solve for C1.

$$C_1 = C_2 \quad 27$$

Equate Eq. 25 and Eq. 26 and solve for b.

$$b = \frac{\frac{\tau_m}{2} * LambertW\left(\frac{2}{\tau_m} * e^{-\left(\frac{2}{\tau_m}(\psi\delta_m + a\tau_m kE - \varepsilon_1 tkE)\right)}\right) + \psi\delta_m + a\tau_m k - \varepsilon_1 tkE}{\tau_m k} \quad 28$$

Solve for the maximum axial pipe displacement, δ_{max}

The distance (a-b) reaches a limiting value as b increases.

Substitute Eq. 25 and Eq. 26 into Eq. 27 and solve for (a-b).

$$(a-b) = \frac{\tau_m\left(e^{-bk}-1\right)^2 + (2\psi\delta_m e^{-bk} + E\varepsilon_1 kt\left(e^{-2bk}-1\right))}{\tau_m k\left(e^{-2bk}-1\right)} \quad 29$$

Solve for the limiting value.

$$\lim_{b\to\infty}(a-b) = \frac{E\varepsilon_1}{\tau_m} - \frac{1}{k} \quad 30$$

This suggests that buried pipe of sufficient length has a limit to axial displacement, δ_{max}.

Apply this limiting value of (a-b) to Eq. 21

$$\delta_{max} = \frac{\delta_m}{2} + \frac{Et{\varepsilon_1}^2}{2\tau_m} \quad 31$$

Observe that δ_{max} is independent of pipe length.

Solve for the limiting value of pipe wall axial stress

The maximum axial stress, σ_{max}, occurs at the value of x causing dσ(x)/dx=0.

Set Eq. 15 equal to 0 and solve for x. The result is x=0. Consequently, σ_{max} occurs at x=0.

Find $\sigma_{max} = \sigma(0)$ using Eq. 13.

$$\sigma_{max} = C_1 + C_2 + \varepsilon_1 E \quad 32$$

A classical thermoelastic material that is fully restrained at both ends, without friction, and subject to temperature or pressure change will experience an axial pressure $\varepsilon_1 E$. A value less than this is intuitively expected since friction on the sides of the pipe assumes some of the stress. Consequently, the sum (C1+C2) $\leq$ 0 is a necessary condition for Eq. 32 to be reasonable.

Experimentation using the equations above reveals that the sum (C1+C2) is negative and approaches 0 as embedment length, b, approaches infinity. Hence, the assumption that $\varepsilon_1 E$ equates to the maximum stress is generally appropriate for a long pipe and otherwise conservative.

Dimensionless Variables

The dependent variables σ(x) and δ(x) may be calculated using Eqs. 13 and 17 for the region 0≤x<b and Eqs. 19 and 21 for the region b≤x≤a. The independent variables are x, δ_m, τ_m, E, t, a, and ε_1: where t and

ε1 are calculated using Eqs. 3 and 4 respectively. Figure 4 exemplifies results of calculations using the following variable values.

δ_m = 5 mm

τ_m = 20 KN/m^2

E = 3000 MN/m^2

t = 25 mm

a = 25 m

ε_1= 0.005

The equations were applied by first calculating the development length (b) using Eq.28. This requires the use of software having the LambertW function. Alternatively, b can be determined by equating Eq. 25 and Eq. 26 and solving iteratively for a value of b that adequately approximates the equality. Subsequently, Eqs. 22 through 26 were used to calculate the constants C1 through C5. Finally, σ(x) and δ(x) were calculated by applying problem variables and constants C1 through C5 to Eqs. 13 and 17 for the region $0 \le x < b$ and to Eqs. 19 and 21 for the region $b \le x \le a$.

Tables can be created that present the results of calculations for dependent variables σ(x) and δ(x) for preselected values of the independent variables. However, many pages of tabularized values could result. For example, consider representing each of the seven independent variables using three values. A total of 3^7=2187 combinations exist.

The number of independent variables can be reduced using dimensional analysis and thereby permit a more condensed presentation of the derived functions. Dimensional analysis was accomplished by the author using methodology described by Langhaar (Langhaar 1951). The following represents a complete set of dimensionless variables.

$\{\sigma(x)/\tau_m, \delta(x)/\delta_m, x/\delta_m, a/\delta_m, t/\delta_m, E/\tau_m, \varepsilon_1\}$

The dimensionless dependent variables are $\sigma(x)/\tau_m$ and $\delta(x)/\delta_m$. The number of independent variables has been reduced from seven to five. Representing each of the five independent variables with three values results in a total of 3^5 = 243 combinations. This is much less than the 2187 combinations needed for the original seven independent variables. Nevertheless, 243 is still many combinations. Furthermore, a table of values does not facilitate a clear understanding of the relationship between variables.

A chart that graph $\sigma(x)/\tau_m$ and $\delta(x)/\delta_m$ for several values of ε_1 and continuously with x would reasonably contain considerably more information and information that is more easily interpreted than tabularized results. Such a chart is presented on Figure 10. Figure 10 presents $\sigma(x)/\tau_m$ and $\delta(x)/\delta_m$ continuously with respect to x and presents results for 5 values of ε1. The chart presents data for single values of dimensionless variables a/δ_m, t/δ_m and E/τ_m. Hence, a single chart represents all but the three dimensionless variables a/δ_m, t/δ_m and E/τ_m by multiple values. A set of charts, consisting of 3^3=27

individual charts, would convey calculated results for 3 values representing each of these three remaining dimensionless variables.

The optimum ranges to be used in plotting sets of charts would depend most significantly on pipe material type, of which there are many. Creating these charts is beyond the scope of this paper.

Application

The conceptual pipe model and its presented solution are intended to characterize general behavior of buried pipe with respect to axial displacement in response to temperature and pressure change. The model and mathematical representation attempts to clarify the way a pipe transfers load to the surrounding embedment. It is expected that the reduced number of independent variables created by dimensional analysis will simplify experimental designs for physical models. The mathematical solution may be applied to practical situations with careful consideration given to the effects of the simplifying and inherent assumptions. Although all assumptions and their effect on the calculated values should be considered when using the equations, special attention must be given to selection of τ_m and δ_m.

Shear stress and normal stress have been assumed to be radially uniform to facilitate a mathematical solution to the problem. However, shear and normal stress will be dependent on the degree of expansion or contraction. Expectedly, both normal stress and shear stress will be lower when the pipe is contracting than when it is expanding, and their magnitude would be a function of the magnitude of change in pipe radius. The magnitude of the rate of change of both the normal and shear stress will not be the same for both the expansion and contraction conditions. Additionally, in cyclic contraction-expansion conditions, it might be expected that the nonuniform alternating behavior of stress and strain in the embedment and at the pipe-embedment interface will cause $\sigma(x)$ and $\delta(x)$ to exhibit hysteresis. Finally, the embedment stress distribution is not uniform about a buried pipe nor is embedment expected to be homogeneous and isotropic as assumed for the model. These deviations from the ideal must be considered when selecting representative values δ_m and τ_m and when interpreting the results of calculations.

Perfectly straight pipe that will not buckle under axial compressive stress is inherently presumed for this model and analysis. Neither condition is expected for long pipe buried at shallow depth. However, application of the results of this work might support understanding that both lateral and axial movement due to pipe bending and associated stress relief would be limited.

Numerical models might be developed to solve the differential equations for a wide range of boundary conditions. Such models may add functions to represent pipe-interface stress as a function of expansion and contraction. The mathematical solution presented herein provides a basis to verify numerical model performance for a simple condition.

Physical models, such as field and laboratory tests on pipe, may be used to evaluate the effects of assumptions inherent to the mathematical solution. Such evaluation would expectedly lead to a better understanding of the nature of pipe-embedment interaction. It has been shown that five independent dimensionless variables can be used to describe the behavior of the simple model of a buried pipe that

experiences a change in temperature and pressure. Hence, these variables should be controlled in experimental designs. Furthermore, it is demonstrated that sets of charts may be created that portray the results of calculations in a meaningful way. Together, these contributions will support the design of experiments that better reveal the nature of pipe-embedment interaction caused by changes in temperature and pressure.

Summary

A mathematical expression describing buried pipe axial displacement caused by changes in temperature and pressure and that is resisted by friction on the pipe-embedment interface is developed to support better understanding of buried pipe behavior and facilitate additional research. The derived equations permit calculation of the upper limit to length change for an unrestrained, long, buried pipe subject to temperature and pressure change. The equations also show that the magnitude of the maximum stress is less than that which is commonly calculated for fully constrained pipe expansion and contraction but approaches the latter value as pipe increases in length.

Problem variables are reduced to dimensionless form and a chart that presents relationships is presented. It is concluded that a set of 27 charts can be used to describe relationships between the two dimensionless dependent variables representing pipe wall stress and displacement and the five independent variables.

The resulting equations must be used with careful consideration given to the simplifying assumptions that were made to facilitate a mathematical solution to the problem. The number of problem variables has been reduced by dimensional analysis. It is hoped that dimensionless problem variables will be helpful in the development of future experimental designs.

x = longitudinal distance from pipe fixed location.
E = elastic modulus representing pipe wall material.
ν = Poisson ratio representing pipe wall material.
D_1 = pipe inside diameter.
D_2 = pipe outside diameter.
A = pipe wall cross-sectional area.
t = transformed pipe wall thickness. Defined herein: $t = A/\pi D_2$.
a = pipe length.
b = development length - the distance from x=0 at which interface friction is fully mobilized.
ΔP= pipe internal pressure change.
ΔT = temperature change.
ΔQ = change in total external stress on pipe.
C = coefficient of linear thermal expansion for the pipe material.
ε1 = approximate change in axial strain due to a changes in temperature and pressure for the condition of unrestricted pipe axial displacement.
ε2(x) = change in horizontal pipe axial strain at x due caused by the buildup of frictional force.
σ(x) = horizontal stress in the pipe wall at x. (tension positive)
δ(x) = horizontal displacement of the pipe at x.
τ(x) = frictional shear stress at the embedment-pipe interface at location x due to pipe axial displacement.
τ_m = maximum interface shear stress ($\psi\ \delta_m$).
δ_m= minimum pipe displacement required to fully mobilize τ_m
δ_{max}= Pipe displacement at the free end of an infinitely long pipe.
ψ = embedment-pipe interface friction constant ($\tau_m / \delta(b)$), dimensions are F/L^3.

$$k = \sqrt{\frac{\psi}{Et}}$$

C_1, C_2, C_3, C_4 and C_5 are constants derived from boundary conditions.

References

Boresi, A.P., Schmidt, R.J. and Sidebottom, O.M., 1985. “Advanced Mechanics of Materials”. New York: Wiley., (p. 499).

ASCE Task Committee on Thrust Restraint Design of Buried Pipelines, 2014. “Research Needs and Recommendations for Testing Thrust Restraint of Buried Pipelines.” *ASCE Pipelines 2014: From Underground to the Forefront of Innovation and Sustainability* (pp. 1805-1815).

Randolph, M.F. and Wroth, C.P., 1978. “Analysis of deformation of vertically loaded piles.” ASCE, *Journal of the Geotechnical Engineering Division*, 104(12), pp.1465-1488.

Motta, E., 1994. “Approximate elastic-plastic solution for axially loaded piles.” ASCE, *Journal of Geotechnical Engineering*, 120(9), pp.1616-1624.

Kraft Jr, L.M., Ray, R.P. and Kagawa, T., 1981. Theoretical t-z curves. ASCE *Journal of the Geotechnical Engineering Division*, 107(11), pp.1543-1561.,

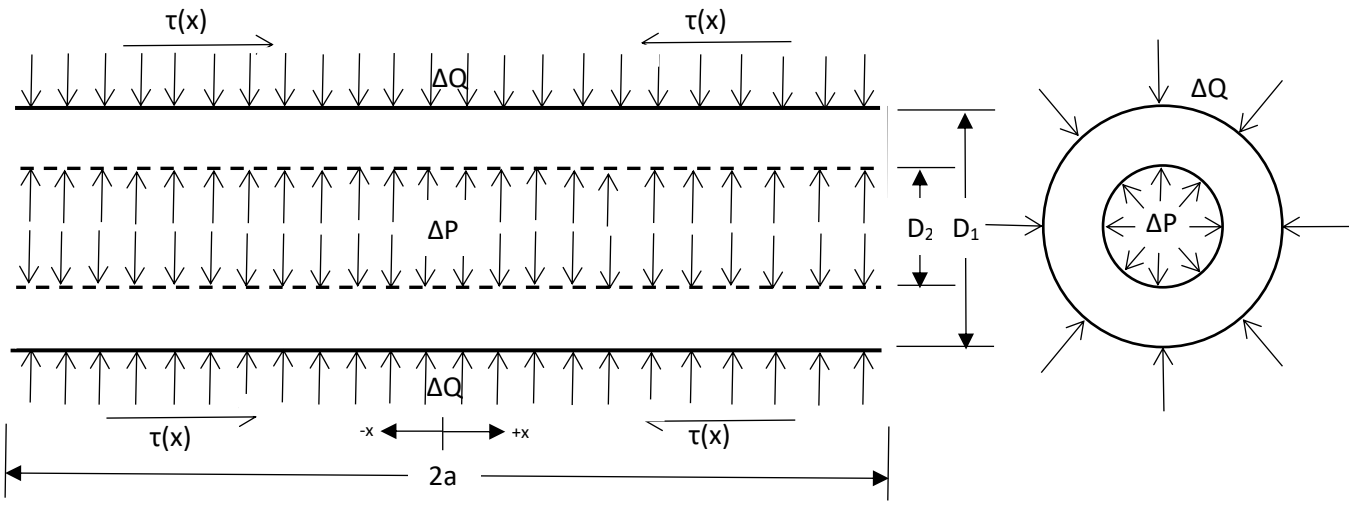

Figure 1. Conceptual pipe model.

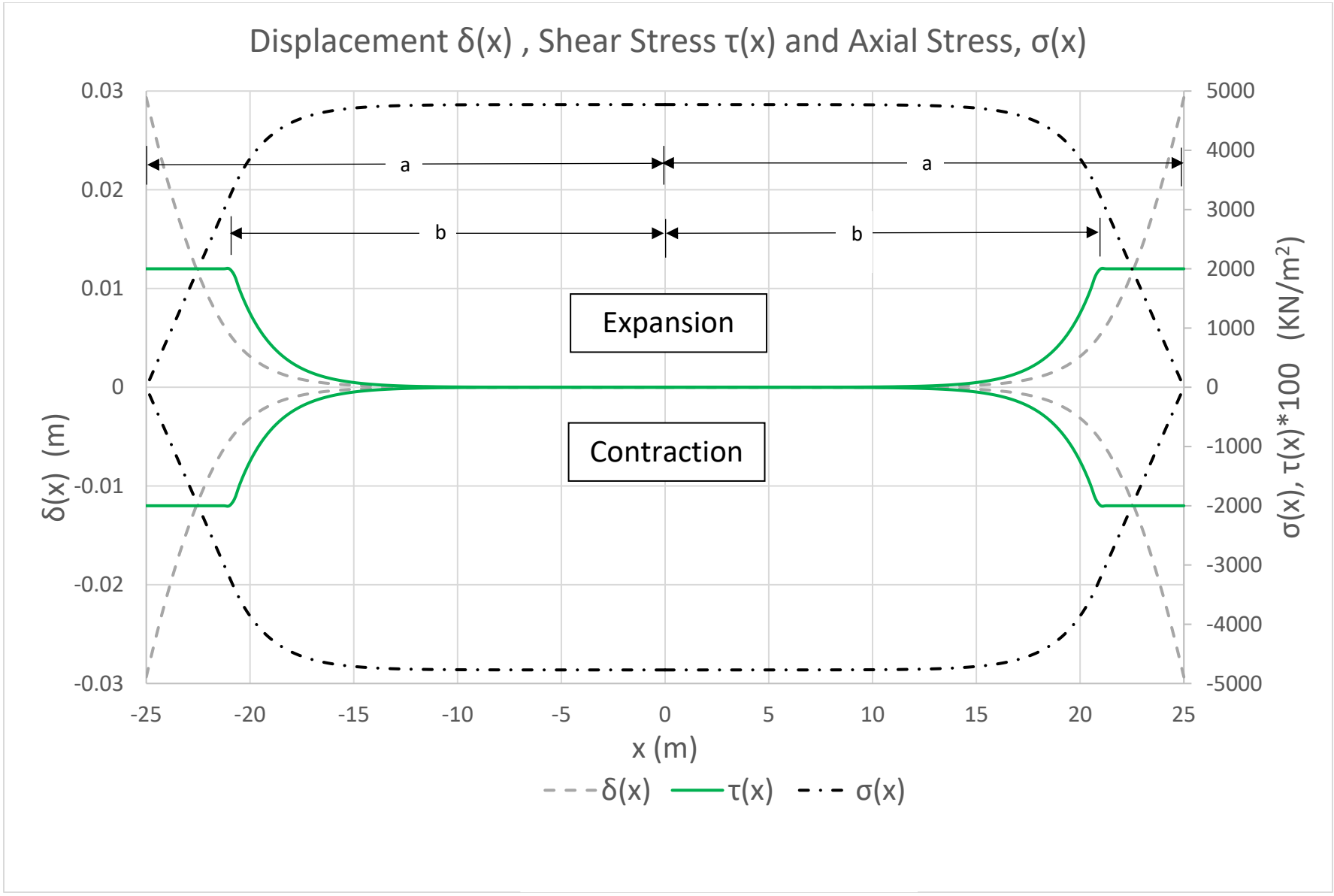

Figure 2. Pipe-interface shear stress τ(x), pipe axial displacement δ(x), pipe axial stress, σ(x), and development

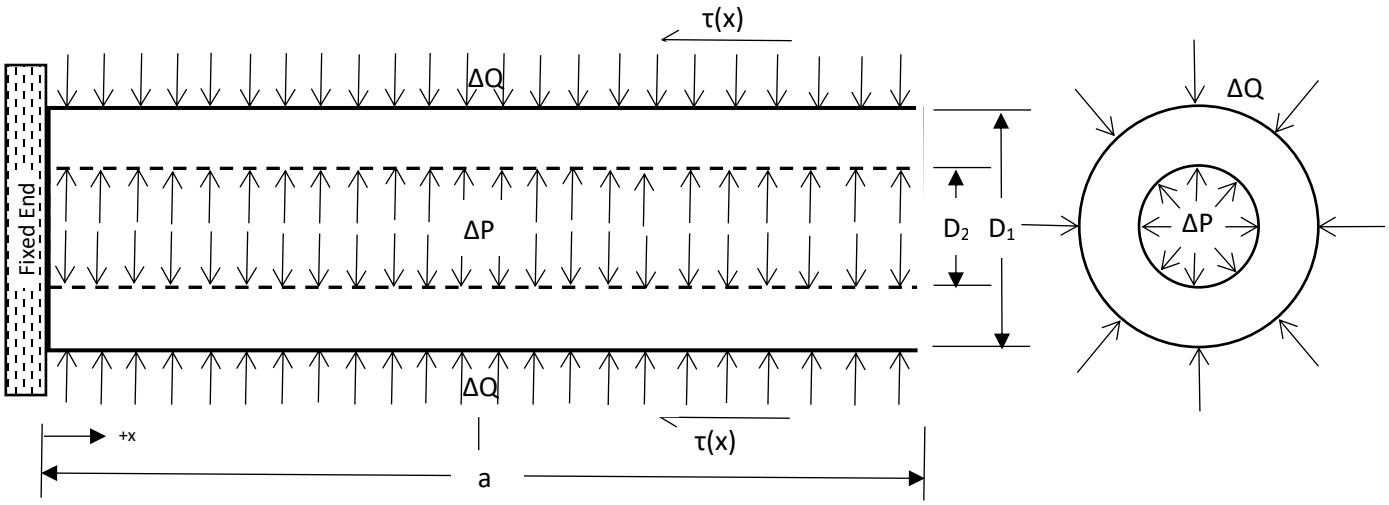

Figure 3. abridged conceptual pipe model.

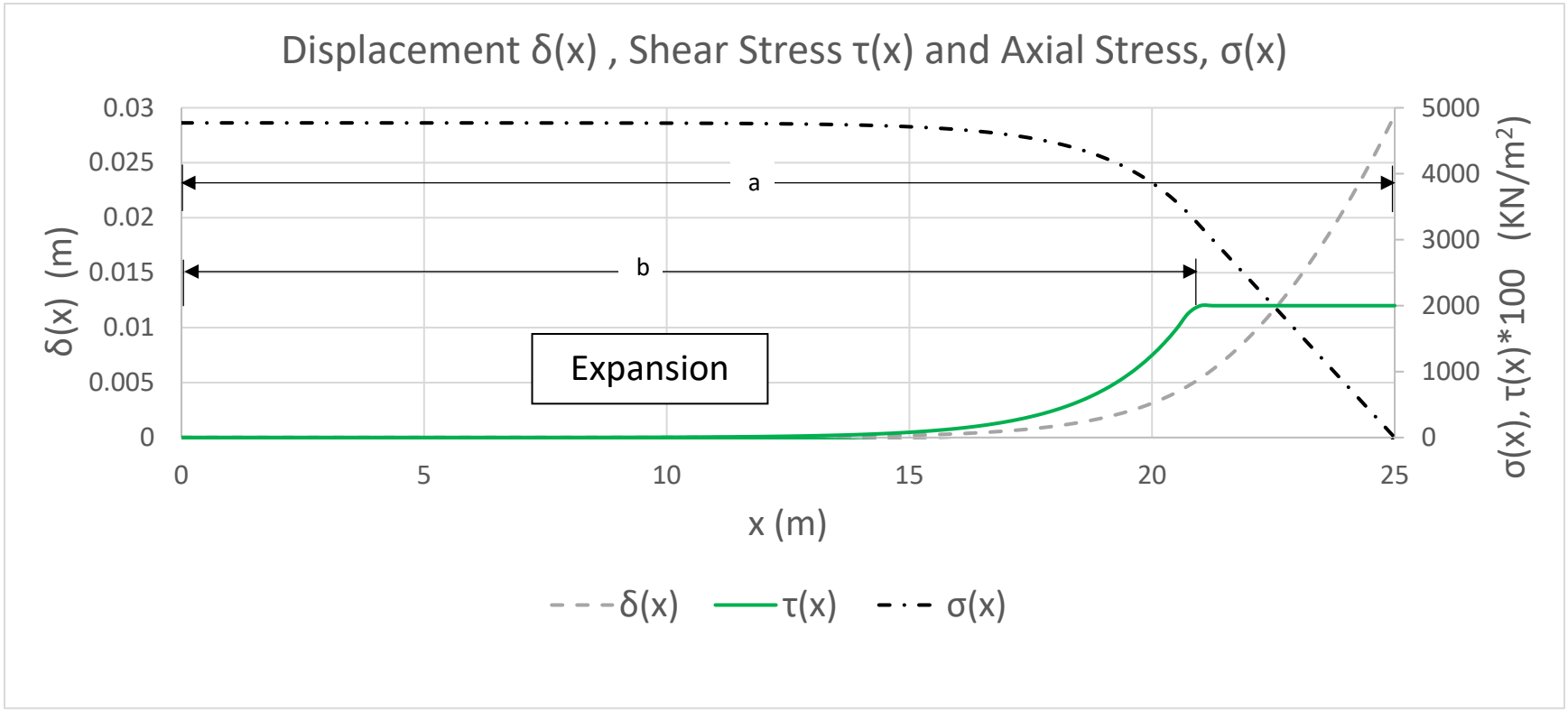

Figure 4. Abridged conceptual pipe model - pipe-interface shear stress τ(x), pipe axial displacement δ(x), pipe axial stress, σ(x), and development length.

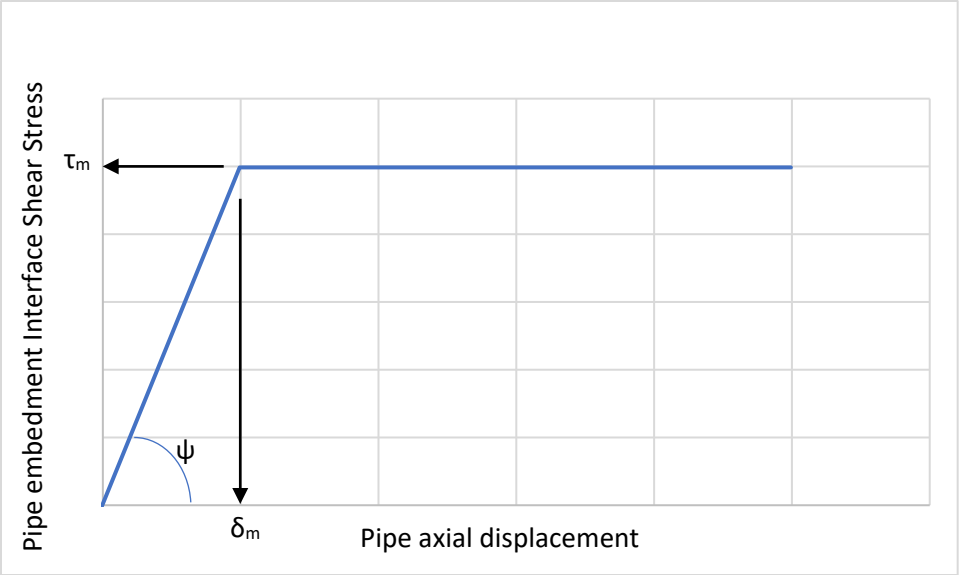

Figure 5. Pipe-embedment interface stick-slip model.

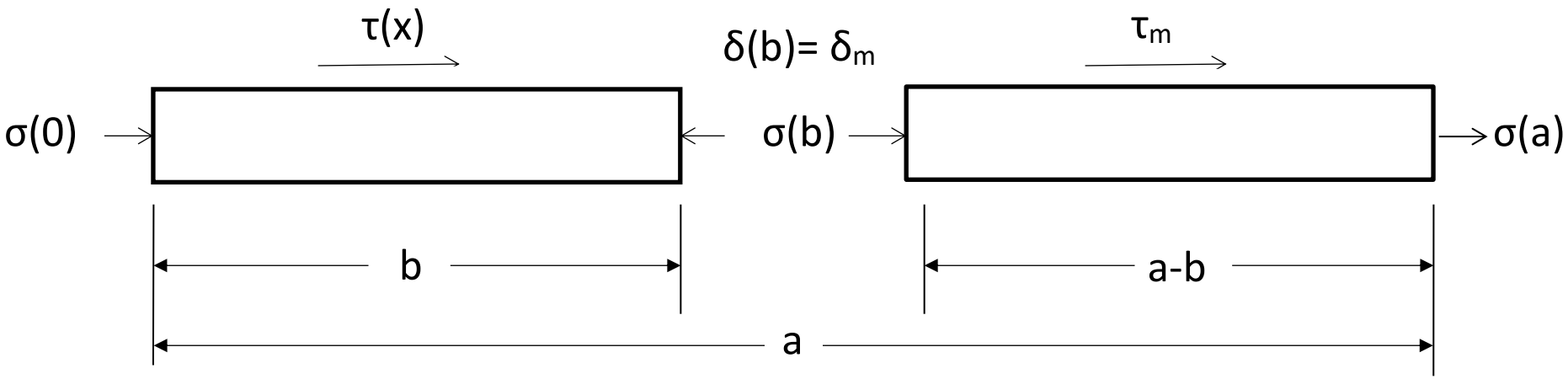

Figure 6. Two parts of the problem.

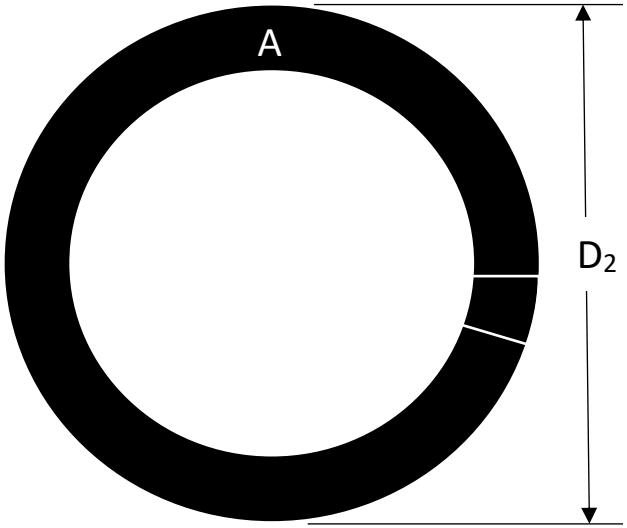

Pipe cross-section.

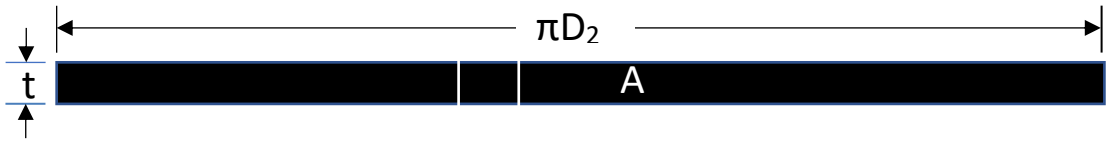

Transformed Pipe Cross-section

Figure 8. Transformation to a one-dimensional problem.

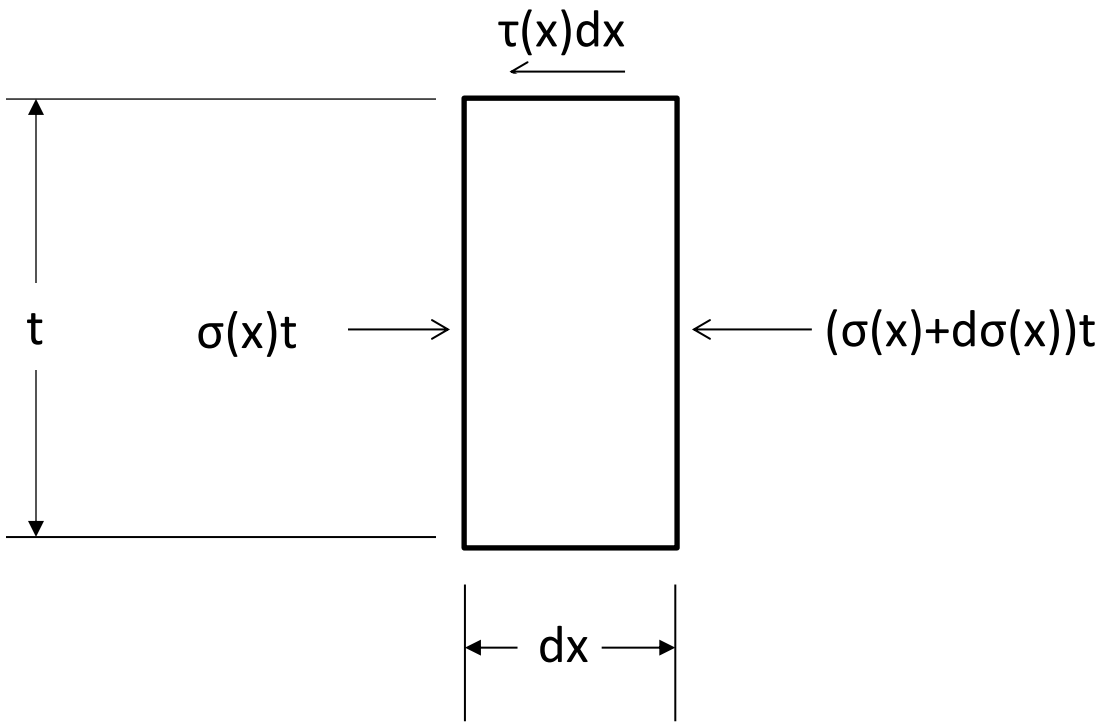

Figure 7. Free Body of infinitesimal axial length (dx) of a unit circumferential length of pipe wall having thickness t.

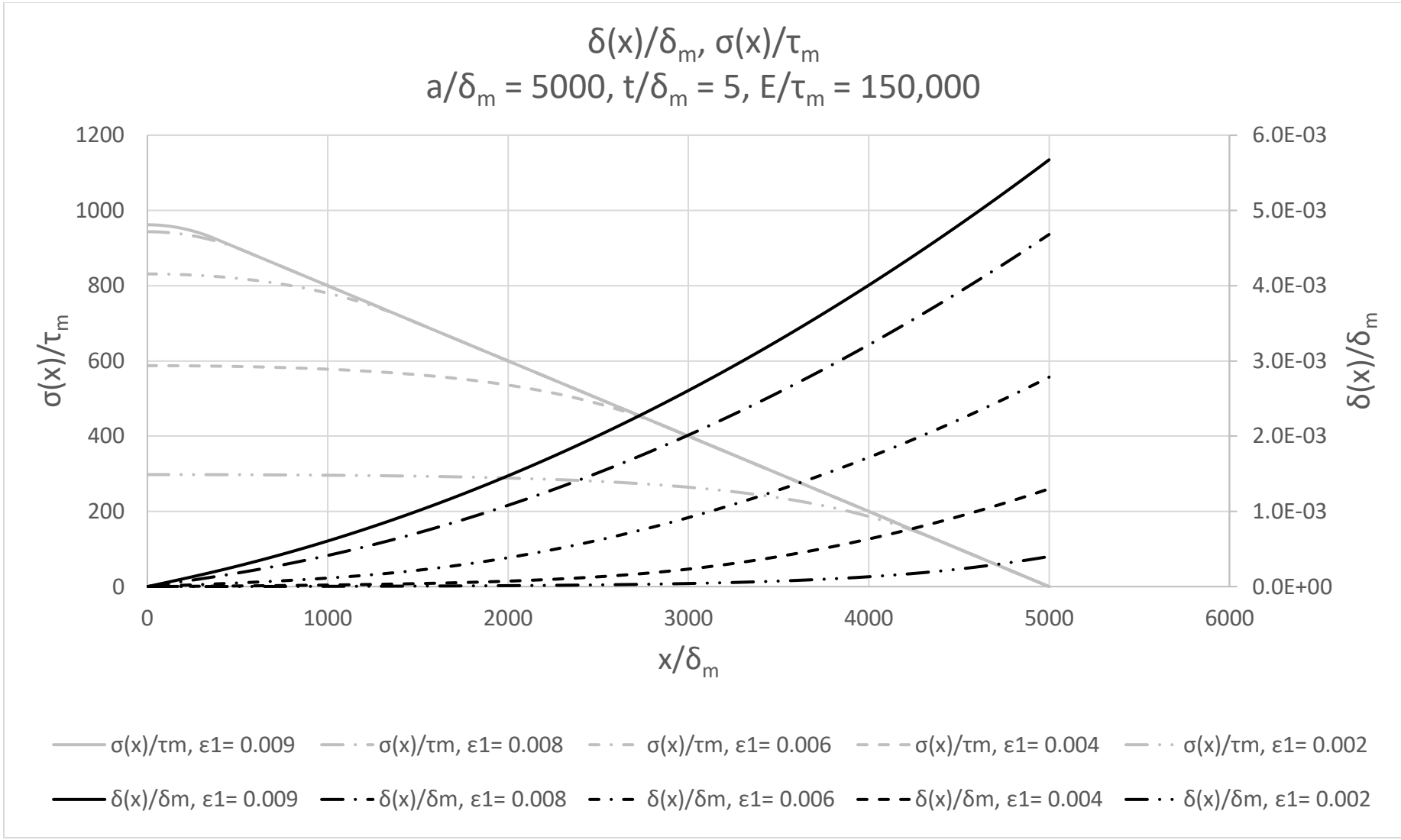

Figure 9. Example chart that presents results of calculations in dimensionless terms.